

OPTIMIZATION OF THE DELTA TECHNIQUE AND APPLICATION TO THE EVALUATION OF ELECTRON-BEAM WELDED TITANIUM AIRCRAFT PARTS

THEODORE E. MATIKAS*

Greek Atomic Energy Commission, P.O. Box 60092, 15310 Agia Paraskevi Attikis, Athens, Greece

(Received 15 May 2001; In final form 9 August 2001)

This paper deals with the development of a non-destructive method for detecting a tight lack-of-fusion defect in electron-beam-welded titanium aircraft parts. The method is based on the ultrasonic delta technique. A combined experimental and theoretical approach is used in this study. The objective of this work is to provide potential users of the technique with guidance for choosing operating frequencies, incidence angles, ultrasonic beam sizes and other experimental parameters so as to maximize the signal-to-noise ratio during use of the delta technique. To achieve its objectives, the paper studies the influence of the material microstructure on the ultrasonic response.

Keywords: Titanium alloys; Ultrasonic delta technique; Non-destructive evaluation; Ultrasonic attenuation; Electron-beam welds

INTRODUCTION

Ultrasonic inspection is one of the most widely used methods to evaluate non-destructively, the integrity of aircraft structural components. It provides a relatively inexpensive, fast, environmental friendly, and reliable way to detect defects and characterize materials and structures. There are many different configurations, ranging from contact ultrasound to laser-generated ultrasound, for performing ultrasonic inspection of aircraft parts, depending on the specific part and the particular conditions of inspection.

Important structural components of the F-22 fighter aircraft are welded, as shown schematically in Fig. 1. These welds are about 4 ft in circumference and there are 20 of these welds, so there are about 80 ft of electron-beam welds in the F-22 aircraft. The parent material for the welds is a Titanium alloy. Boeing is committed to use the delta ultrasonic technique to inspect electron-beam welds in the F-22 in regions where the two surfaces are parallel. This will account for about 95% or more of the welds in the F-22 aircraft. Boeing's delta technique is used to inspect the central half of the weld thickness, which is about half an inch. Boeing is using a single, contact, water-coupled transducer for insonification, generating a mode-converted, 60° shear wave.

*Tel.: +30-1-650-6752. Fax: +30-1-650-6748. E-mail: matikas@otenet.gr

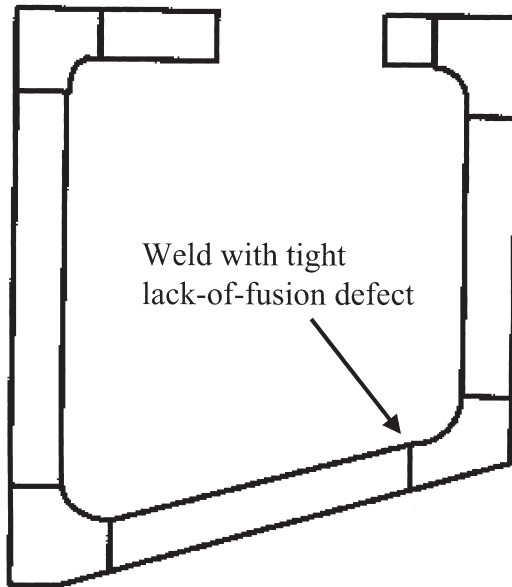


FIGURE 1 Schematic of electron-beam-welded titanium F-22 part with tight lack-of-fusion defects.

PRINCIPLE OF THE DELTA TECHNIQUE

The principle of operation of the ultrasonic delta technique is shown in Fig. 2. An emitter-transducer is used at a specific angle θ_i to induce elastic waves in the solid. Longitudinal waves and mode-converted shear waves are then propagating downward. The upward radiated wave, generated by scatter from material grains in the area of the weld, is finally received by the receiver transducer situated at a distance d from the emitter. The receiver can be either a single transducer or an array of transducers. For instance, Boeing is using a set of 15 receiving transducers. Analysis of the received refracted wave from the weld will assist in detecting defects, such as lack-of-fusion.

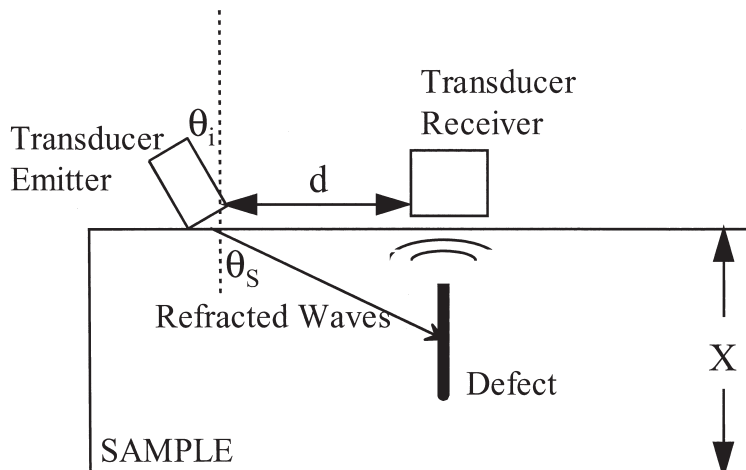


FIGURE 2 Ultrasonic delta technique configuration.

The downward-radiated elastic wave cannot be used in curved regions (primarily corners) where the two surfaces are not parallel. In those curved non-parallel regions, only the direct upward-radiated wave can be used. However, since the upward-radiated wave is very weak, the signal-to-noise ratio is small and the signal is difficult to detect. Therefore, there is a need to optimize the technique for the reception of the direct, upward-radiated elastic wave. Using a pitch-catch shear wave technique could be an effective way for inspecting the curved portions of the electron-beam welded parts, however, this technique is difficult to apply in a field situation.

OPTIMIZATION OF THE DELTA TECHNIQUE

As shown in Fig. 2, the delta technique consists of only two parts: (a) transmission/refraction of ultrasonic waves in the solid; and (b) reception of the elastic waves by the receiver. The reception part of the waves is passive. Thus, for inspecting a particular titanium weld, the optimization of the downward-refracted wave amplitude is essential for optimizing the received signal amplitude, using the configuration of the delta technique. To maximize flaw detectability in the weld, it is therefore necessary to optimize ultrasonic emission parameters such as ultrasonic frequency, angle of incidence, and distance between emission and reception transducers in order to obtain maximum refracted signal amplitude.

Modeling the Refraction of An Ultrasonic Wave in the Weld

There are three basic competing mechanisms affecting the refracted wave amplitude: (a) mode conversion effect according to wave refraction laws; (b) shear-wave polarization effect, which corresponds to the effective reflected shear-wave component; and (c) attenuation of the shear refracted waves.

Mode Converted Shear Waves

Using the Snell's law and wave propagation principles, the downward-radiated refracted-wave amplitude T is given by the following expression:

$$T = \frac{-4c_{2S}^2 q \sqrt{1 - q^2}}{N c_{2L}^2} \quad (1)$$

where

$$N = 4qs \left(\frac{c_{2S}}{c_{2L}} \right)^2 \sqrt{1 - q^2} \sqrt{1 - s^2} + [1 - 4s^2(1 - s^2)] + \frac{\rho_1 c_1 \sqrt{1 - q^2}}{\rho_2 c_{2L} \cos \theta_i} \quad (2)$$

$$q = \sin \theta_i \frac{c_{2L}}{c_1} \quad (3)$$

$$s = \sin \theta_i \frac{c_{2S}}{c_1} \quad (4)$$

θ_i is the angle of incidence, c_1 and ρ_1 , are the sound velocity and the density of the coupling medium (water), c_{2L} and c_{2S} , the velocity of longitudinal and shear elastic waves in the weld, respectively, and ρ_2 is the density of the weld.

Equation (1) shows that the amplitude of the refracted wave depends on the elastic properties of the weld (density, ultrasonic velocities), and the angle of incidence of the ultrasonic beam.

From the configuration shown in Fig. 2, and assuming that a mode-converted shear wave transmitted in a solid plate of thickness X at an angle θ_s interacts with a defect in the weld situated in the middle of the plate, the distance d between the emitter and the receiver is given by:

$$d = \frac{X}{2} \tan \theta_s \quad (5)$$

Effective Shear Wave Component

In the configuration shown in Fig. 3, an ultrasonic transducer produces elastic waves in a solid material. The waves are incident on a slot that simulates the defect in the weld and then received by a second transducer positioned in the configuration used in the delta technique. It is obvious that when a contact, vertically polarized (vibrating normal to the detector) shear wave transducer, coupled to the test block using special coupling, is used as an emitter (Fig. 3a), a radiated wave with an amplitude greater than the background noise is received by the longitudinal transducer located above the slot. However, when the emitter is a horizontally polarized, shear wave transducer (Fig. 3b), no radiated wave (greater than the noise level) can be detected by the longitudinal receiver. Figure 3c shows the real configuration of the delta technique. The mode-converted shear wave transmitted in the solid can be resolved into vertical and horizontal components. The horizontal component vibrates normal to the face of the slot, so, there is no radiated wave detectable by the longitudinal receiver, whereas, the vertically polarized component of the shear wave interacts with the slot and produces a significant radiated wave. This vertically polarized component of the angled shear wave is therefore the “effective shear wave component” denoted by “ s ” and is given by Eq. (4).

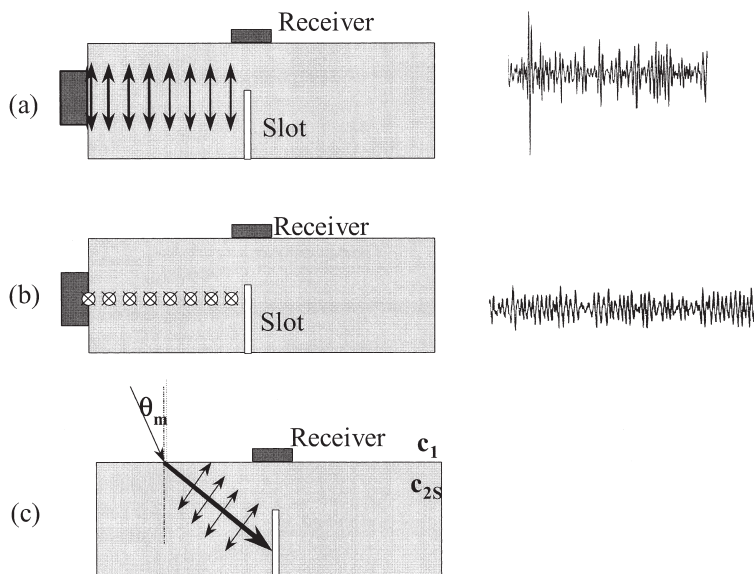


FIGURE 3 Effective shear wave component: (a) vertically polarized shear waves and received signal by delta technique; (b) horizontally polarized shear waves and received signal by delta technique; and (c) mode converted shear waves.

A methodology based on the closely related time of flight diffraction (TOFD) technique could also be used to predict the magnitude of the diffracted wave as a function of angle and wave polarization. The TOFD technique uses two transducers, one of which detects diffracted signals from crack tips [1–3].

Effect of Attenuation on the Received Amplitude

The attenuation due to scattering influences the transmitted amplitude in the solid and therefore, the received amplitude using the delta technique. The effect of attenuation is described by the term:

$$M = \exp \left[-\alpha \frac{X}{\sqrt{s^2 - 1}} \right] \quad (6)$$

where α is the attenuation coefficient in the solid, X is the thickness of the solid plate and s is the effective shear wave component.

To illustrate the effect of attenuation on the transmitted amplitude, Fig. 4 shows the dependence of the reflected amplitude of a mode-converted shear wave in titanium on the angle of incidence. The solid line shows the reflected amplitude without taking into account the attenuation, whereas the dotted line shows the reflected amplitude when the attenuation effect is taken into account. Three cases of solids with different attenuation are shown: a case of low attenuation, $\alpha = 10$ dB/m, is shown in Fig. 4a; a case of medium attenuation, $\alpha = 30$ dB/m, is shown in Fig. 4b; and a case of high attenuation, $\alpha = 75$ dB/m, is shown in Fig. 4c. The density of titanium is $\rho = 4.52$ kg/m³ and the longitudinal and shear wave velocities are: $c_{2L} = 6040$ m/s and $c_{2S} = 3100$ m/s, respectively. The thickness of the solid plate was taken as: $X = 25.4$ mm. The first, θ_1 , and the second, θ_2 , critical angles are then calculated from the equations:

$$\theta_1 = a \sin \left(\frac{c_1}{c_{2L}} \right) \quad (7)$$

$$\theta_2 = a \sin \left(\frac{c_1}{c_{2S}} \right) \quad (8)$$

and found to be 14.2° and 28.5° , respectively, and the Rayleigh angle is $\theta_R = 30.5^\circ$.

For a solid with 10 dB/m attenuation coefficient, the maximum received amplitude of mode-converted shear waves in titanium is obtained for an angle of incidence $\theta_i = 26^\circ$, as shown in Fig. 4a. This angle corresponds to the optimum angle of incidence for the delta technique. The refracted angle of shear waves is therefore $\theta_s = 66.7^\circ$ and the distance between the emitter and the receiver, given by Eq. (4), is $d = 29$ mm.

For a solid with 30 dB/m attenuation coefficient, the maximum received amplitude of mode-converted shear waves in titanium is obtained for an angle of incidence between 16° and 24° , as it can be observed from the plateau shown in Fig. 4b. The refracted angle of shear waves is therefore between 35.2° and 58.4° and the distance between the emitter and the receiver is between 9 and 20.5 mm.

For a solid with high attenuation coefficient of 75 dB/m, the maximum received amplitude of mode-converted shear waves in titanium is obtained for an angle of incidence $\theta_i = 16^\circ$, as it can be observed from Fig. 4c. The refracted angle of shear waves is therefore $\theta_s = 35.2^\circ$ and the distance between the emitter and the receiver is $d = 9$ mm.

Please note that in Fig. 4a–c, for presentation purposes only, the magnitude of the function $T \cdot M$ was multiplied by a factor: 3 in the case of 10 dB attenuation; 6 in the case of 30 dB attenuation; and 30 in the case of 75 dB attenuation.

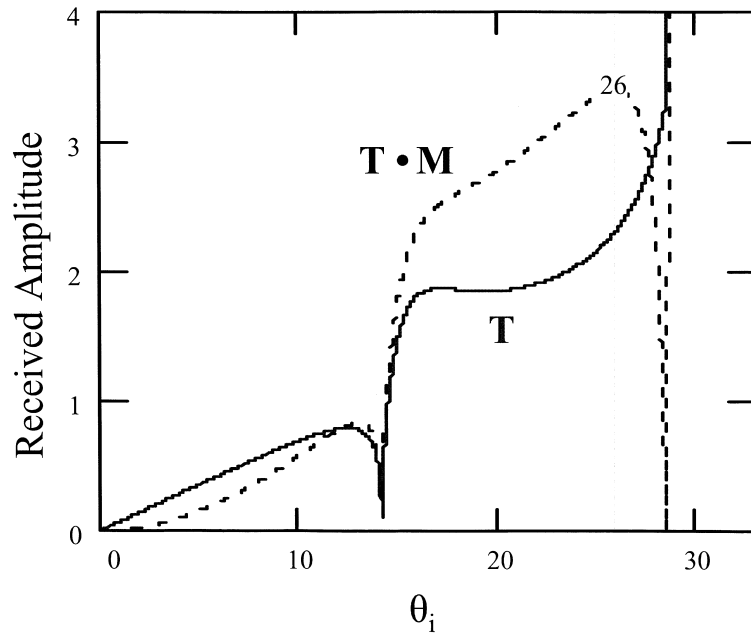


FIGURE 4(a)

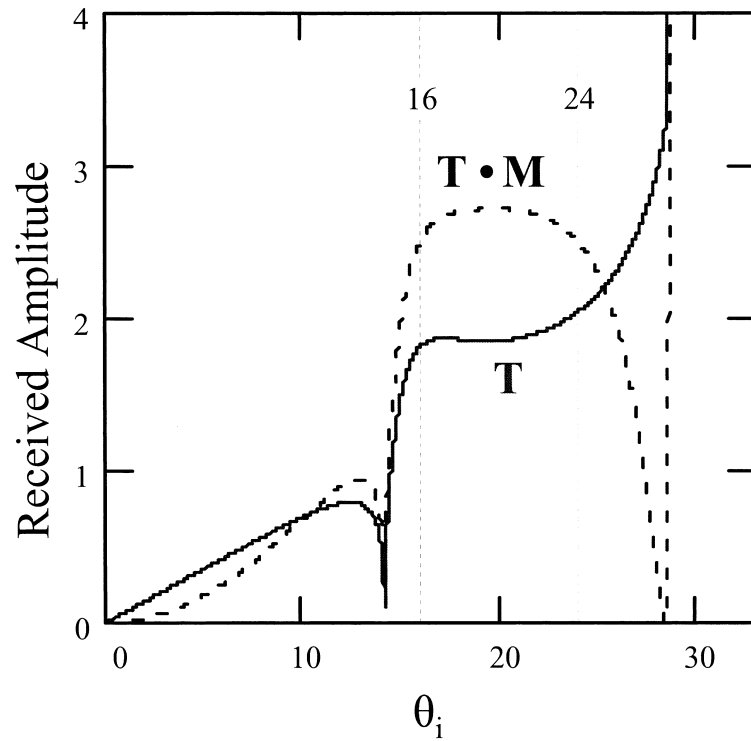


FIGURE 4(b)

Figure 5 shows for comparison the three competing effects. The combined effect for a specific value of attenuation coefficient is given by the relationship:

$$F = T \cdot M \cdot s \quad (9)$$

where F denotes the combined received amplitude.

It is evident from the above analysis that, for the optimization of experimental parameters in delta technique configuration used for evaluating titanium welds, it is essential to take into account the attenuation effect, which is particularly significant in titanium. For this reason, the following section presents a study of the attenuation of shear waves in titanium alloys.

ATTENUATION IN TITANIUM

Titanium alloys are highly inhomogeneous multi-phase materials. Attenuation in titanium alloys is due to: (a) scattering of ultrasound at grain boundaries where acoustic impedance changes abruptly; and (b) absorption due to conversion of acoustic energy to heat. Anisotropic attenuation occurs in case of random orientation of grains. In the case of coarse grain materials, in which grain size is comparable to the wavelength (localized inhomogeneity), a mode conversion phenomenon occurs. At each grain boundary, the incident wave splits into various longitudinal and transverse modes and can be visualized geometrically. In this study, the absorption contribution to attenuation is assumed to be negligible.

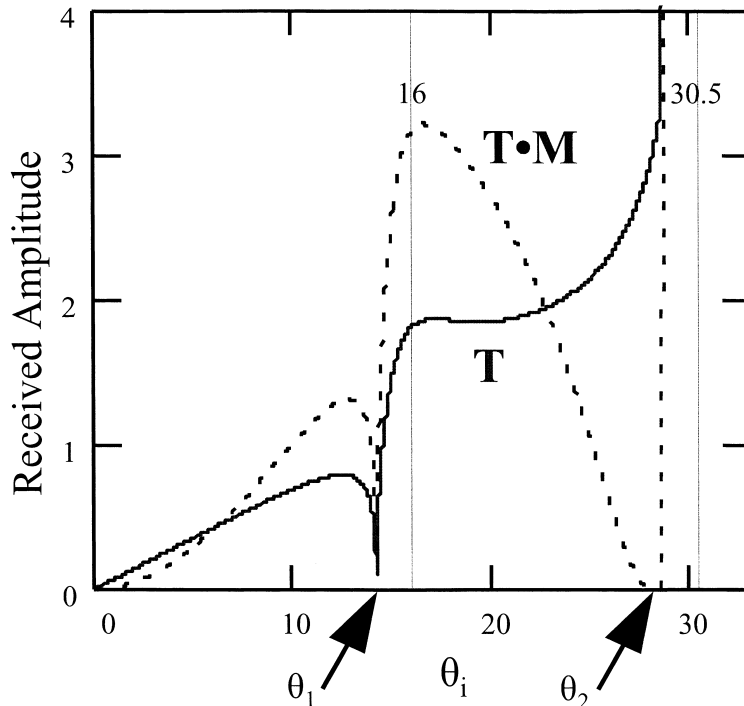


FIGURE 4(c)

FIGURE 4 Effect of attenuation on ultrasonic wave propagating in the weld: (a) case of low attenuation $\alpha = 10$ dB/m; (b) case of medium attenuation $\alpha = 30$ dB/m; and (c) case of high attenuation $\alpha = 75$ dB/m.

Theory

The attenuation coefficient of a polycrystalline material such as titanium is defined by:

$$\alpha(f) = \alpha_a(f) + \alpha_s(f) \quad (10)$$

where α_a is the absorption coefficient and α_s is the grain scattering coefficient due to energy dispersion of the traveling waves. The effective velocity of wave propagation is determined by the elastic moduli and the orientation of the grains. If a preferred grain orientation exists, the medium can become elastically anisotropic as a whole, so that the velocity is a function of the direction of propagation [4].

The scattering is dependent on the type, size, and orientation of the grains as well as the mode of incident waves. The grain scattering problem has been solved by Lifshitz *et al.* for an isotropic, equiaxed, homogeneous polycrystalline material [5]. Three distinct mechanisms of attenuation caused by grain scattering exist: (a) Rayleigh, when the wavelength $\lambda > 2\pi D_g$; (b) stochastic, when $\lambda \sim 2\pi D_g$; and (c) diffusion, when $\lambda < 2\pi D_g$, and D_g is the average equivalent grain diameter with an approximation of spherical grains. The analytical solutions of scattering coefficients for each of these cases may be found in the literature [6–9]. For example, Merkulov obtained the general solutions of both Rayleigh and diffusion scattering for the special cases of cubic and hexagonal metals [6]. An equivalent theoretical analysis was performed by Bhatia and Moore for Rayleigh scattering in the case of orthorhombic materials [7]. In general, the attenuation due to grain scattering for all the different cases can be written in the form:

$$\alpha(\lambda) = \frac{a_1}{\lambda} + a_2 \frac{D_g^3}{\lambda^4} \quad \text{when } \lambda > 2\pi D_g \quad (11)$$

$$\alpha(\lambda) = \frac{b_1}{\lambda} + b_2 \frac{D_g}{\lambda^2} \quad \text{when } \lambda \sim 2\pi D_g \quad (12)$$

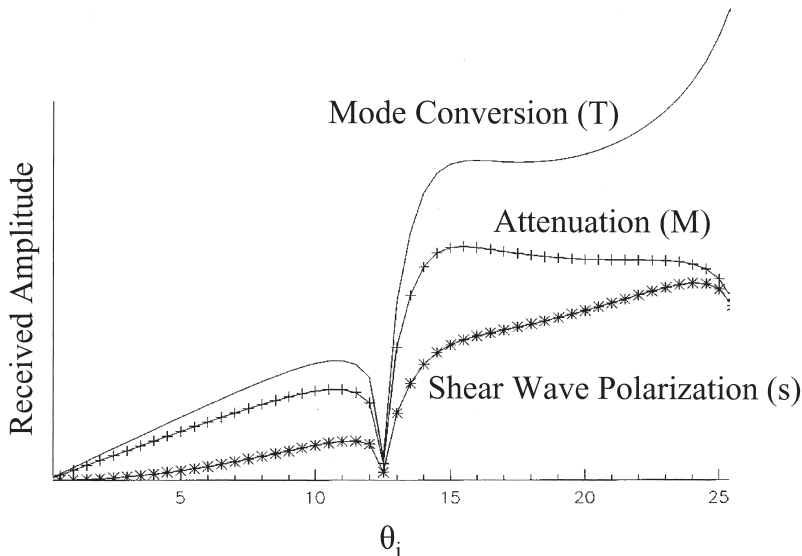


FIGURE 5 Comparison of the three competing effects, T , M , and s , for the same value of attenuation coefficient.

$$\alpha(\lambda) = \frac{c_1}{\lambda} + \frac{c_2}{\lambda^2} + \frac{c_3}{D_g} \quad \text{when } \lambda < 2\pi D_g \quad (13)$$

where a_1, b_1, c_1, c_2 are absorption coefficients and a_2, b_2, c_3 are scattering coefficients.

Thus, from Eqs. (11)–(13), it is reasonable to define that as: when $\lambda > 2\pi D_g$ (Rayleigh scattering),

$$\alpha_s(\lambda) = C_1 \frac{D_g^3}{\lambda^4} \quad (14)$$

when $\lambda \sim 2\pi D_g$ (stochastic scattering),

$$\alpha_s(\lambda) = C_2 \frac{D_g}{\lambda^2} \quad (15)$$

and, when $\lambda < 2\pi D_g$ (diffusion scattering),

$$\alpha_s(\lambda) = C_3 \frac{1}{D_g} \quad (16)$$

where C_1, C_2 and C_3 are constants.

Hence, the degree of scattering is a function of the wavelength, λ , of the incident ultrasonic waves and the average grain dimension D_g . It should be noted that the relationships Eqs. (14)–(16) are valid only if the grain shape can be approximated as spherical (i.e. equiaxed) [10]. Finally, reference should be given to the recent work of Panetta *et al.* [11,12] who have studied the influence of microstructurally induced fluctuations on back-scattered signals and performed measurements of ultrasonic attenuation in titanium alloys.

Experimental Method

For the measurement of shear wave attenuation in titanium, a method is proposed based on the configuration shown in Fig. 6. First, the ultrasonic velocities are measured in the titanium

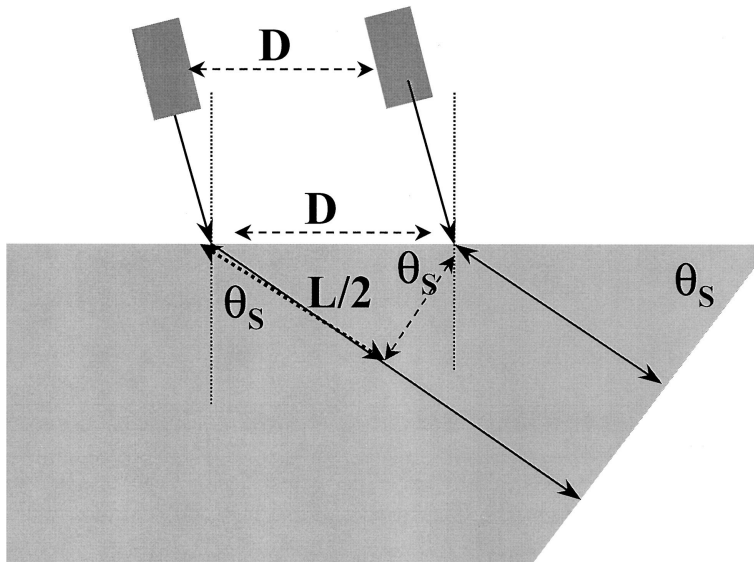


FIGURE 6 Measurement of shear wave attenuation in titanium.

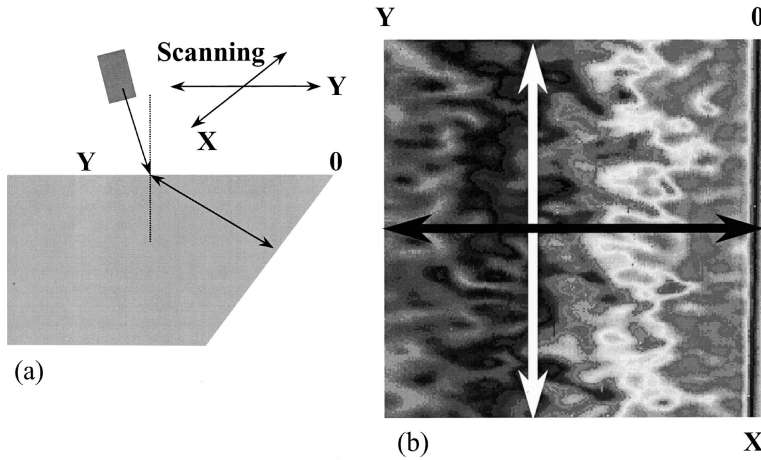


FIGURE 7 Effect of attenuation for a particular direction of wave propagation: (a) experimental configuration; (b) corresponding back-reflected shear wave C-scan image showing variation in ultrasonic amplitude due to attenuation and changes in local microstructure.

alloy under examination and the shear wave refraction angle θ_S is calculated. An angled block of the same material is made with an angle equal to θ_S in one side, as shown in Fig. 6. The specimen is immersed in water and an immersion ultrasonic transducer is used in pulse-echo mode. Mode converted shear waves are transmitted and back-propagated in the solid and finally received by the same transducer. The transducer is displaced at a fixed distance D and two measurements are obtained. The difference in propagation path of the shear waves for displacement D of the transducer is fixed:

$$L = 2D \sin \theta_S \quad (17)$$

The anisotropic attenuation of shear waves can then be calculated by measuring the decrease in amplitude of the shear wave traveling a specific distance L . It must be noted that the measurements are always done in the same direction. Therefore, an advantage of this technique is that it is also applicable in the case of anisotropic attenuation, which is frequently the case in titanium alloys.

Measurement of Attenuation Due to Scattering

Using the configuration described in the previous section, the attenuation was measured in the titanium sample. Figure 7a shows the experimental configuration. A 10 MHz planar ultrasonic transducer operating in pulse-echo mode was used in immersion to scan an area of the sample in the X and Y directions as shown in Fig. 7a. The angle of incidence was 20° and the shear wave refraction angle was $\theta_S = 45.7^\circ$. The acquired C-scan of the back-propagated shear waves is shown in Fig. 7b. Figure 7b shows the amplitude of the signal received from the transducer. The X and Y directions correspond to the same directions shown in Fig. 7a. The variation of the ultrasonic amplitude along the X direction (light color line) is due to variation in the local material microstructure. The origin 0 corresponds to the edge of the titanium block. The variation along the Y direction (dark color line) shows the effect of attenuation. As the transducer is moved away from the edge, the shear wave path in the solid increases which results in the decrease in the signal received by the transducer.

Figure 8 shows the received signals of three separate lines A, B, and C corresponding to three lines of the C-scan as shown in Fig. 8d. The line A was closer to the edge of the titanium

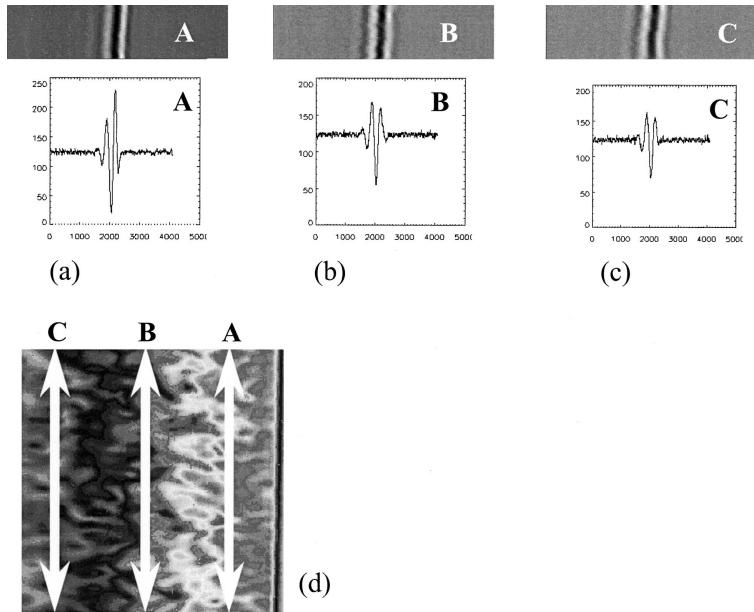


FIGURE 8 Received signals in delta technique configuration from three separate lines A, B, and C corresponding to three lines of the C-scan shown in (d): (a) B-scan and representative A-scan from line A (closer to the edge of the sample); (b) B-scan and representative A-scan from line B; (c) B-scan and representative A-scan from line C (far from the edge of the sample) and (d) C-scan showing the location of the three line-scans.

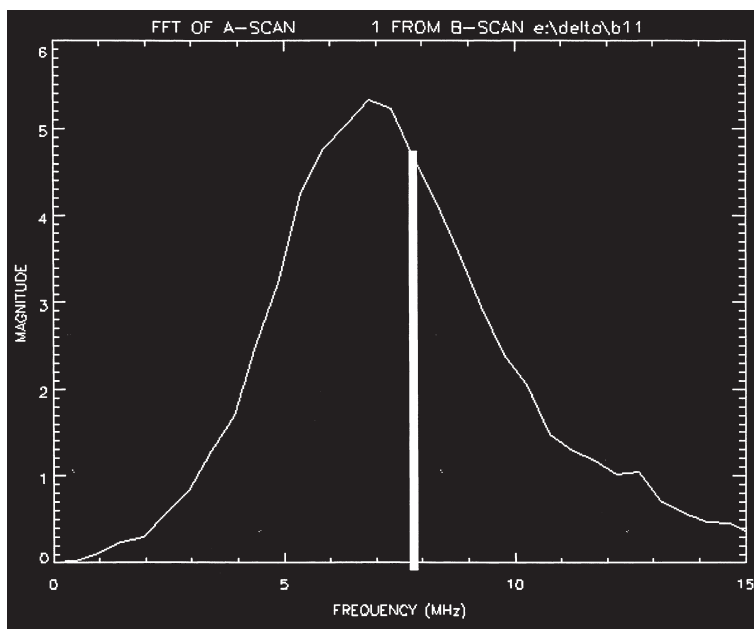


FIGURE 9 FFT of an A-scan and magnitude of the received signal at a given frequency.

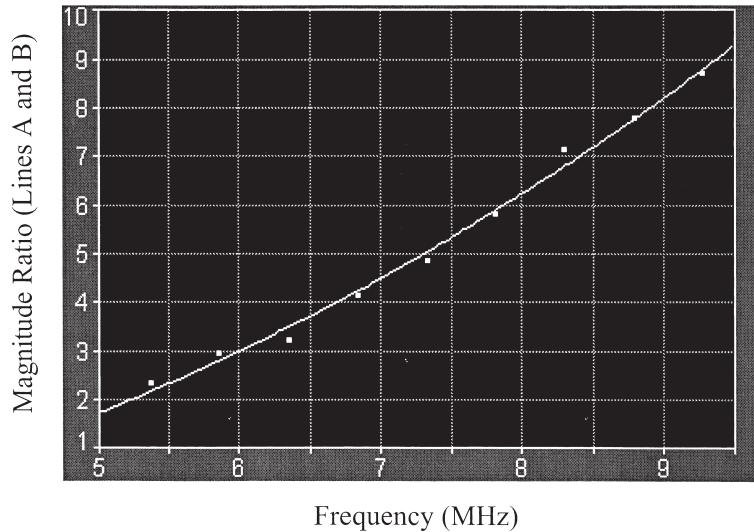


FIGURE 10 Ratio of magnitudes between the lines A and B (difference in the relative path of shear wave 20.5 mm) as a function of frequency.

block, which corresponds to the shorter path of shear waves in the solid. The lines, B and C correspond to two positions of the transducer apart from each other at a distance $D = 10$ mm. This leads to $L = 0$ mm for A, $L = 20.5$ mm for B, and $L = 41$ mm for C. The corresponding B-scans (line scans) and a representative A-scan (point signal) for each line are shown in Fig. 8a–c. As it was expected, the amplitude for the line A (shorter path of shear waves) is greater than the amplitude corresponding to line B, and this one is also greater than the amplitude corresponding to line C (longer path of shear waves).

Analysis and Results

Measurements of two lines were sufficient for getting the shear wave attenuation coefficient in the titanium block. An FFT was performed for each A-scan of the B-scan. The average magnitude at a given frequency (Fig. 9) was then obtained. The ratio of the magnitudes from the two lines at a given frequency was then plotted as a function of frequency. To prove the consistency of the results in this study, three lines were used and two independent measurements were compared which gave similar results.

Figure 10 shows the ratio of magnitudes between the lines A and B (difference in the relative path of shear wave 20.5 mm) as a function of frequency. The fitting curve follows the equation:

$$y = a + bx^2 \quad (18)$$

where $a = -1.2$ and $b = 0.115$.

Figure 11 shows the ratio of magnitudes between the lines B and C (same difference in the relative path of shear wave, 20.5 mm, as between the lines A and B) as a function of frequency. The fitting curve satisfies the same Eq. (18) with $a = 2.6$ and $b = 0.125$. This demonstrates the consistency of the measurements, which give a similar b for both situations, where the difference in the relative path of the shear waves is the same.

For a frequency range of 5–9 MHz for example, the corresponding wavelength of shear waves in the titanium block is $\lambda = 340\text{--}620$ μm . Given the fact that the average grain size was measured to be $D_g \sim 70$ μm , the parameter $2\pi D_g$, which plays an important role in

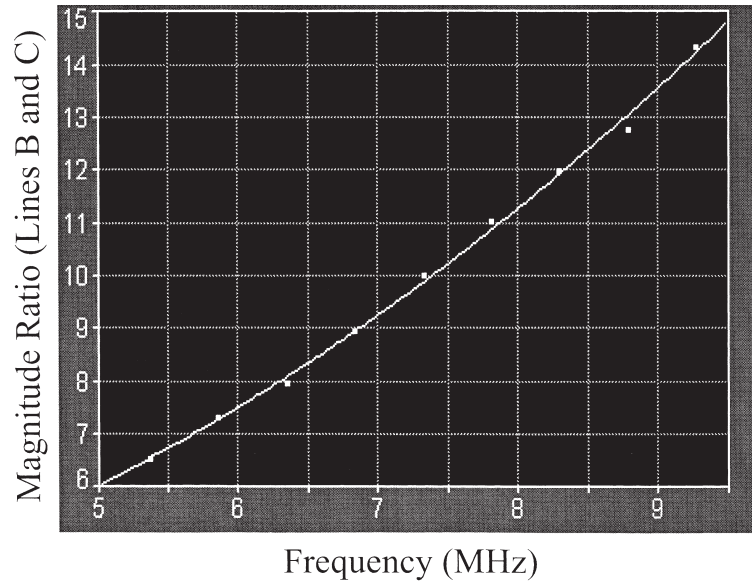


FIGURE 11 Ratio of magnitudes between the lines B and C (difference in the relative path of shear wave 20.5 mm) as a function of frequency.

defining the type of attenuation as discussed in the “Theory” section, is about $400 \mu\text{m}$. This means that $2\pi D_g \sim \lambda$, which corresponds to stochastic scattering.

The attenuation coefficient is therefore given by Eq. (15), which becomes:

$$\alpha = (b/L)f^2 \text{ (dB/mm)} \quad (19)$$

where $b = 0.12$ is the parameter measured in Figs. 10 and 11, $L = 20.5 \text{ mm}$ is the difference in relative path of shear waves, and f is the ultrasonic frequency.

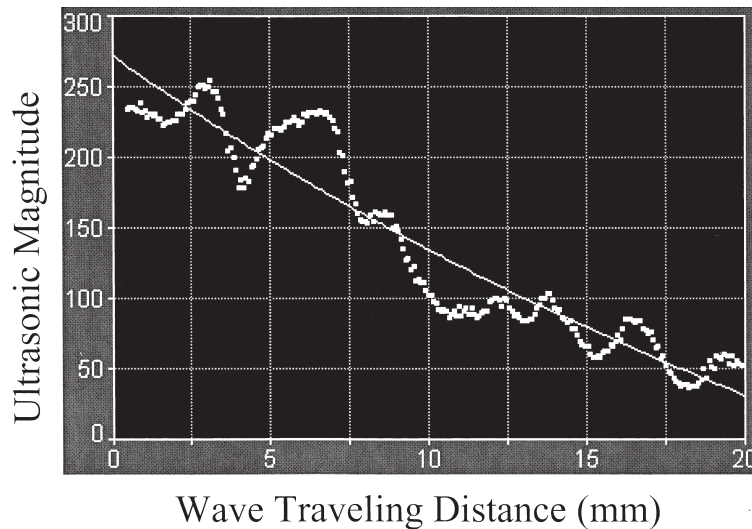


FIGURE 12 Magnitude of the 2 MHz received signal as a function of the traveling distance of shear waves in the titanium block.

From Eq. (19), and for an ultrasonic frequency of 2 MHz, the measured attenuation coefficient of the titanium block is, $\alpha = 0.023$ dB/mm.

A second method for calculating the attenuation coefficient in the titanium block was also used to verify the consistency of the results. Figure 12 shows the magnitude of the received signal for ultrasonic frequency of 2 MHz as a function of the traveling distance of shear waves in the titanium block (along the dark line in the Y direction in Fig. 7). There is some irregularity in the curve due to the local material microstructure. The fit of the curve however is an indication that the deduced wave attenuation mechanism may be a reasonable assumption.

$$y = \exp[-x/a] \quad (20)$$

where $a = 43.5$. The attenuation coefficient is therefore $\alpha = 1/a = 0.023$. This implies that the two methods: Eqs. (19) and (20), give the same value for the attenuation coefficient.

Equation (19), which has been used to predict attenuation as a function of frequency for the titanium block, is only valid for a specific direction of wave propagation (anisotropic attenuation). To map and describe the anisotropic attenuation in the material, a calibration block of conical shape of angle θ_s (or θ_l) can be used, depending on the measurement of attenuation for a particular wave mode, transverse or longitudinal. By rotating the transducer, a polar plot of attenuation as a function of angle (anisotropic attenuation) can be obtained.

OPTIMIZATION OF PARAMETERS FOR THE DELTA TECHNIQUE

Based on the above study, the optimum experimental parameters for the delta technique can be determined.

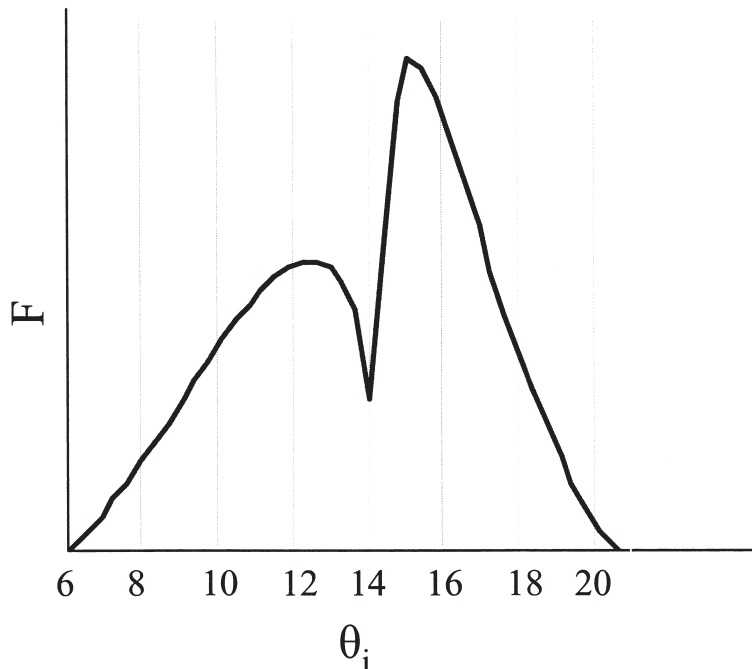


FIGURE 13 Combined ultrasonic amplitude received by the transducer in delta technique configuration as a function of the angle of incidence.

Figure 13 shows the combined ultrasonic amplitude F , as defined by Eq. (9), received by the transducer in delta technique configuration as a function of the angle of incidence θ_i . The plate thickness is $X = 25.4$ mm and the ultrasonic frequency is 7 MHz. The attenuation coefficient is calculated to be $\alpha = 0.26$ dB/mm. From the analysis, it was found that the optimum angle of incidence is $\theta_i = 15^\circ$ (as shown in Fig. 13). The emitter and the receiver should be positioned at an optimum distance $d = 8.1$ mm, calculated using Eq. (5).

CONCLUSION

The optimization of a promising ultrasonic technique to evaluate the integrity of titanium weld is presented in this paper. The delta technique is a non-destructive method used for detecting internal defects in plate-like structures. An application of the technique is the non-destructive evaluation of tight lack-of-fusion defects in electron-beam-welded titanium parts used in the F-22 aircraft. Optimizing the delta technique helps users of the method for choosing the best experimental parameters. It was found that the attenuation plays a significant role for optimal application of the delta technique. A method for measuring the shear wave attenuation is proposed in this paper. The methodology presented here provides for optimal reception of the ultrasonic signal and for maximizing flaw detection using the ultrasonic delta technique. This is achieved by determining the optimum operating frequency, angle of incidence, and relative positions of the emitter and the receiver transducers.

Acknowledgements

This research was performed on-site at the NDE Branch, Air Force Research laboratory, Wright-Patterson Air Force Base, Ohio, USA.

References

- [1] Ogily, J.A. and Temple, J.A.G. (1983) "Diffraction of elastic waves by cracks: application to time of flight inspection", *Ultrasonics*, 259–269.
- [2] Norris, A.N. and Achenbach, J.D. (1984) "Elastic wave diffraction by a semi-infinite crack in a transversely isotropic material", *Quart. J. Mech. Appl. Math.* **37**, 565–580.
- [3] Budreck, D.E. and Achenbach, J.D. (1988) "Scattering from three-dimensional planar cracks by the boundary integral equation method", *J. Appl. Mech. Trans.* **55**, 405–412.
- [4] Papadakis, E.P. (1968) "Ultrasonic attenuation caused by scattering in polycrystalline media", In: Mason, W.P., ed, *Physical Acoustics* (Academic Press, New York) **Vol. 4-B**, pp 269–328.
- [5] Lifshitz, E.M. and Parkhomovskii, G.D. (1950), *Zh. Eksperim. i Teoret. Fiz.* **20**, 175–182.
- [6] Merkulov, L.G. (1956), *Soviet Phys.-Tech. Phys. (English Transl.)* **1**, 59–69.
- [7] Bhatia, A.B. and Moore, R.A. (1959), *J. Acoust. Soc. Am.* **31**, 1140–1142.
- [8] Morse, P.M. and Ingard, K.V. (1968) *Theoretical Acoustics* (McGraw-Hill, New York).
- [9] Meeker, T.R. and Meitzler, A.H. (1964) In: Mason, W.P., ed, *Physical Acoustics* (Academic Press, New York) **Vol. 1-A**, pp 111–167.
- [10] Krishnamurthy, S., Matikas, T.E. and Karpur, P. (1997) "Role of matrix microstructure in the ultrasonic characterization of fiber-reinforced metal matrix composites", *J. Mater. Res.* **12**, 754–763.
- [11] Panetta, P.D., Margetan, E.J., Yalda, I. and Thompson, R.B. (1996) "Ultrasonic attenuation measurements in jet-engine titanium alloys", *QNDE. Rev. Prog.* **15B**, 1735.
- [12] Panetta, P.D., Margetan, E.J., Yalda, I. and Thompson, R.B. (1997) "Observation and interpretation of microstructurally induced fluctuations of back-surface and ultrasonic attenuation in titanium alloys", *QNDE. Rev. Prog.* **16B**, 1547.